

The Effect of Pulsed Sliding Surface Discharges on Supersonic Airflow past a Thin Wedge in Shock Tube

I. V. Mursenkova*, A. S. Sazonov, and Yu. Liao

Faculty of Physics, Moscow State University, Moscow, 119992 Russia

*e-mail: murs_i@physics.msu.ru

Received October 11, 2017

Abstract—The influence of ~ 300 -ns pulsed sliding surface discharges on supersonic airflow with $M = 1.2$ – 1.5 past a thin wedge has been studied in a shock tube at 0.12 – 0.14 kg/m³ gas density. It is established that inhomogeneity of the airflow–density field near the wedge leads to changes in the discharge current geometry and the structure of surface–discharge glow. The dynamics of discharge–initiated shock waves disturbing the quasi-stationary flow past the wedge was studied by the method of shadow visualization. It is shown that shock waves from intense surface–discharge channels in front of the wedge and behind its rear part can produce nonstationary action on the flow past the wedge surface, which lasts for up to 120 μ s after the discharge pulse.

DOI: 10.1134/S1063785018020256

The modification of a flow field past a body with the aid of surface plasma actuators can lead to changes in the characteristics of high-speed flows as a result of the interaction of plasma with the gas medium [1–5]. In solving the problems of supersonic plasma gasdynamics, these devices are of considerable interest due to advantages such as fast response and possibilities of optimum arrangement on aerodynamic surfaces [1, 3, 5].

The present work was aimed at experimental investigation of the (i) influence of nanosecond pulsed sliding surface discharges on supersonic airflow past a thin wedge in shock tube with $M = 1.2$ – 1.5 and (ii) character of shock-wave processes after the discharge pulse.

The investigation was carried out in a setup with a shock tube containing a discharge chamber shaped as a 24×48 -mm rectangular channel [3, 6]. The opposite side walls of the discharge channel were made of plane-parallel silica-glass plates; the top and bottom walls bore planar systems of electrodes generating surface discharges (Fig. 1a).

Experiments were performed in air at pressures within 2.7 – 53.3 kPa, in which supersonic flows with velocities of 630 – 950 m/s were formed behind plane shock waves generated at Mach numbers $M = 2.6$ – 3.6 . Under these conditions, a single homogeneous supersonic cocurrent flow with $M = 1.2$ – 1.5 and duration of 300 – 500 μ s is formed in the discharge chamber (closed by a contact surface) [7, 8]. A thin dielectric (Caprolon) wedge with a height of 24 mm, a length of 49 mm, and a width of 8 mm with an opening angle of

$\sim 9^\circ$ was mounted in the discharge channel and oriented towards the shock wave at a zero angle of attack for the flow behind. After the shock-wave diffraction on the wedge, stationary supersonic flow was established within 100 μ s with a wedge-shaped bow shock [8] and a duration of ~ 200 – 400 μ s. At this stage of flow, surface discharges (plasma sheets) with a 100×30 mm area were initiated on the top and bottom walls of the discharge channel (Fig. 1a).

A sliding pulsed surface discharge develops in a thin layer of gas near the dielectric surface upon the application of voltage to the electrode system of special configuration playing the role of plasma actuator

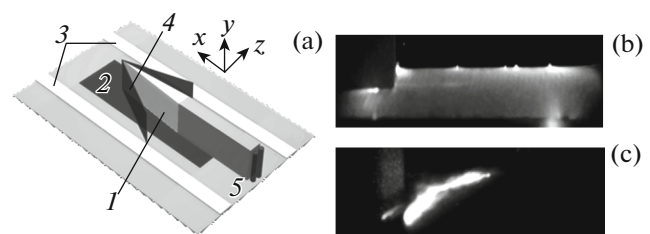


Fig. 1. (a) Scheme of airflow around the wedge in the discharge chamber: (1) wedge, (2) discharge region, (3) silica-glass plates, (4) bow shock wave, and (5) vortex region. (b, c) Photographs of the surface-discharge glow on the bottom wall of the discharge channel in (b) quiescent air and (c) the vortex region behind the wedge in supersonic flow with $M = 1.27$ and a gas density of 0.12 kg/m³. The airflow moves left to right (bottom wall of the wedge is seen on the left). The last image was obtained with an optical filter transmitting light with 405 -nm wavelength.

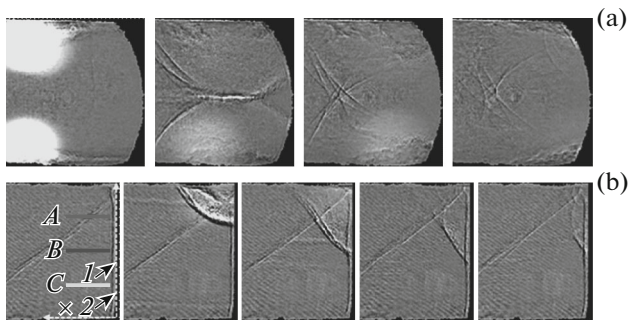


Fig. 2. Sequential shadow images of the flow field after discharge: (a) behind the wedge rear plane under experimental conditions corresponding to Fig. 1c (bright regions in the first frame show discharge sections, while left boundaries of frames coincide with the wedge rear plane (interframe period 7 μ s, exposure time 1 μ s)); (b) in front of wedge nose in supersonic flow with $M = 1.44$ at gas density 0.14 kg/m³; dark band (1) at the right-hand boundaries of frames coincides with the wedge nose; line (2) on the left is the bow shock-wave front (interframe period 9 μ s, exposure time 1 μ s). The airflow moves left to right; letters A–C denote lines corresponding to flow sections at $y = 18, 12,$ and 6 mm, respectively.

[2, 3, 6, 7]. The applied voltage pulse with a front steepness of $\sim 10^{11}$ V/s had an amplitude that varied within 16–25 kV at a current amplitude of ~ 1 kA and duration of ~ 300 ns. The reduced electric field reached $E/N \sim 10^{-19}$ V m², where E is the field intensity and N is the concentration of gas molecules. In quiescent air with a density of 0.12–0.14 kg/m³, the discharge has the form of planar linear segments sliding over the dielectric surface and forming a continuous layer (plasma sheet) with thickness below 0.5 mm [6, 7]. These discharges generate semicylindrical shock waves that interact with each other. The presence of the wedge in the discharge plane led to partial overlap of discharge segments, while the plasma layer in the remaining part remained homogeneous in the case of quiescent air (Fig. 1b). In supersonic flow at Reynolds numbers of $\sim 10^5$, the plasma-layer thickness was comparable with that of a boundary layer at the walls of discharge channel. The characteristics of flow near the surface influence the character and geometry of developing sliding discharge [7].

In these experiments, we used the shadow visualization method to study the flow field near the wedge during a period of time between the arrival of a plane shock wave to the wedge nose and the termination of a homogeneous cocurrent flow and for monitoring the dynamics of motion of the shock-wave configurations for 200–400 μ s after discharge. The optical system of shadow visualization formed a parallel probing beam 40 mm in diameter that was directed perpendicular to glass walls of the discharge channel. The shadow images were recorded by a Photron Fastcam SA5 camera with a frequency of up to 150 000 frames per second at an exposure time of 1 μ s. At the same time, photo-

graphic images were recorded through the glass walls of the discharge channel by Canon EOS 550D and Nikon D50 cameras oriented at small angles relative to the plane of plasma sheets. Since the discharge-glow duration was below 500 ns, the photographic images gave “instantaneous” gasdynamic patterns of emission distribution from surface discharges. The synchronization of processes and switching of recording equipment was governed by signals from piezoelectric sensors of pressure in the shock tube.

There were two series of experiments, in which the wedge was (i) arranged symmetrically at the center of discharge channel and (ii) elongated by an inset so that the rear part would protrude out of the discharge region (Fig. 1a). In the latter case, we have studied the effect of surface discharges on the flow in front of the wedge nose. The rear dielectric (Caprolon) inset had the shape of a parallelepiped with a height of 24 mm, a length of 52 mm, and width of 8 mm. In the case of stationary supersonic flow past the wedge in the channel, the flow field has a bow shock wave in front of the wedge, shock waves reflected from the walls, oblique shocks, and a vortex region of reduced density behind the rear edge (Fig. 1a). The vortex-region size was on the order of the wedge rear-side width in the transverse direction.

The development of pulsed discharge in an inhomogeneous density field proceeds so that the breakdown is initiated in the region of maximum values of reduced electric field E/N [7, 9, 10]. The results of discharge-glow monitoring in the first series of experiments showed that discharges were developing only in the vortex region of reduced density at a distance of 6–9 mm from the rear side of wedge and had the form of one or more curvilinear high-intensity channels (Fig. 1c) symmetric in the upper and lower plasma sheets. The glow of discharge channels was nonuniformly distributed along their length: the intensity was lower in the central region than at the edges, and the central part was bent toward the wedge. Therefore, the energy deposited in the flow is redistributed both over the surface and in the length of the discharge channel. The shadow images of the flow field behind the discharge in this case showed that intense shock waves originated from both upper and lower discharges with velocities up to 1500 m/s at the initial stage (Fig. 2a). These waves moved symmetrically toward and interacted with each other and affected the flow past the rear part of the wedge for 30–40 μ s after discharge. The shape of the shock-wave fronts deviated from semicylindrical, and the resulting shock-wave configuration propagated at a velocity close to that of the airflow.

In the second series of experiments, we studied the discharge glow and flow field at the wedge nose after discharge initiation. In these experiments, the surface-discharge glow was found to be inhomogeneous. At a quasi-stationary stage of the flow, a single intense-dis-

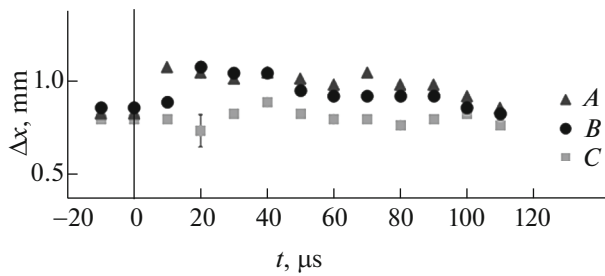


Fig. 3. Temporal variation of the average deviation of the bow shock wave in flow sections at $y = 18$ (A), 12 (B), and 6 mm (C) as indicated in the first frame of Fig. 2b ($t = 0$ corresponds to the moment of discharge).

charge channel usually occurred in front of the wedge at a position dependent on the flow conditions. The discharge channel generated a strong shock wave that moved with the flow toward the wedge and significantly influenced the flow field in front of the edge. The set of shadow images in Fig. 2b shows how the shock wave originating from the upper plasma sheet of the discharge channel moves upside down, decays with time, and shifts rightward with the flow (frames 3–5, 10–40 μs after discharge). This shock wave and the flow behind interact with the bow shock in front of the wedge, change its shape and position, and, hence, modify the regime of the flow past the wedge.

Analysis of the obtained schlieren images reveals the dynamics of the bow shock-wave deviation (distance from the wedge nose to the shock-wave front), which is shown in Fig. 3. Figure 2b indicates flow sections in the channel (lines A–C) along which the images were processed and the deviation of bow shock from the wedge nose was measured. The undisturbed stationary deviation in the flow with $M = 1.43 \pm 0.03$ amounted to 0.85 ± 0.05 mm at an airflow density of 0.14 kg/m^3 . Interaction of the bow shock wave with the shock wave coming from the discharge channel led to a local increase in the deviation, with subsequent return to the stationary unperturbed value within 70–120 μs . The value of deviation averaged over this series of experiments exceeded the unperturbed value by $25 \pm 5\%$ and remained increased for ~ 70 μs along line A and for ~ 40 μs along line B (Fig. 3).

In concluding, the results of our investigation showed that the initiation of pulsed sliding surface dis-

charges in the supersonic airflow ($M = 1.2\text{--}1.5$) past thin wedge leads to changes in the geometry of discharge current and the flow field downstream the discharge. The glow emission from plasma of sliding discharge in supersonic airflow behind the obstacle is localized in a curvilinear inhomogeneously glowing channel, the position of which depends on the geometry of the appearing vortex region. It is established that shock waves coming from intense discharge channels can act for a prolonged period of time upon flow behind the rear side of the wedge and the bow shock wave in front of it, producing nonstationary deviation of the bow shock. Data of high-speed shadow imaging showed that the duration of nonstationary action of the localized energy supply significantly exceeds the discharge-pulse duration and can reach up to 120 μs after discharge.

Acknowledgments. This study was supported by the Russian Foundation for Basic Research, project no. 17-08-00560.

REFERENCES

1. J. J. Wang, K. Choi, L. Feng, T. N. Jukes, and R. D. Whalley, *Prog. Aerosp. Sci.* **62**, 52 (2013).
2. K. D. Bayoda, N. Benard, and E. Moreau, *J. Appl. Phys.* **118**, 063301 (2015).
3. I. A. Znamenskaya, D. F. Latfullin, A. E. Lutskii, and T. V. Mursenkova, *Tech. Phys. Lett.* **36**, 795 (2010).
4. A. A. Zheltovodov and E. A. Pimonov, *Tech. Phys.* **58**, 170 (2013).
5. T. A. Lapushkina, A. V. Erofeev, and S. A. Ponyaev, *Tech. Phys.* **56**, 616 (2011).
6. I. A. Znamenskaya, D. F. Latfullin, A. E. Lutsky, I. V. Mursenkova, and N. N. Sysoev, *Tech. Phys.* **52**, 546 (2007).
7. I. Belysheva, I. Mursenkova, and A. Chvyreva, *J. Phys.: Conf. Ser.* **516**, 012021 (2014).
8. T. V. Bazhenova and L. G. Gvozdeva, *Unsteady Interactions of Shock Waves* (Nauka, Moscow, 1977) [in Russian].
9. Yu. P. Raizer, *Gas Discharge Physics* (Springer, Berlin, 1991; Intellekt, Dolgoprudnyi, 2009).
10. I. A. Znamenskaya, I. E. Ivanov, M. K. Kul'kin, I. V. Mursenkova, and A. S. Sazonov, in *Proc. of the 44th International Zvenigorod Conference on Physics of Plasma and Controlled Thermonuclear Synthesis* (Moscow, 2017), p. 278.

Translated by P. Pozdeev